# A 30 GHz Steerable Patch Array Antenna for Software-Defined Radio Platforms

Marc Jean\*, Ectis Velazquez\*, Xun Gong, and Murat Yuksel Electrical and Computer Engineering University of Central Florida

marc1988@Knights.ucf.edu, Ectis.Velazquez@knights.ucf.edu, xun.gong@ucf.edu, murat.yuksel@ucf.edu

Abstract—We present design and simulation of a beamsteering patch antenna array that operates at 30 GHz. The antenna design includes feeding lines needed for connection to a software-defined radio (SDR) platform. Phase differences on the feeding lines are minimal and the impact of the feeding network on the gain is negligible at the operational frequency. Each patch element of the antenna has an associated 5-bit phase shifter allowing fine granularity beam-forming capability out of the array. The simulation results show that the antenna attains very similar gain patterns to ideal ones.

Index Terms—beamforming, mmWave, phase shifters, SDR

#### I. Introduction

As the wireless community is looking for more bandwidth, millimeter wave (mmWave) bands, 28-100 GHz, are deemed the next best resource to tap into. Design of antennas accessing mmWave bands is of high demand as there is a growing need for affordable, beam-steerable and software-controllable mmWave antennas. Among other alternatives, patch array antennas have a number of beneficial features, such as beamforming capabilities, low cost of manufacturing, and high directivity. As a result, antenna arrays [6] are being used in popular applications, such as the Internet-of-Things and Multiple-Input and Multiple-Output communication systems. These types of systems are applying intelligent beamforming methods to make spectrum access more efficient in 5G networking [11], [13]. Further, beamforming can be used to realign the radiation pattern between the transmitter and receiver, which decreases overall system noise [14]. In antenna arrays, beamforming is achieved by altering the phase values of the signals at the transmitting or receiving ports of the individual antenna elements [7]. By changing these phase values, the direction of the radiated signal can be controlled by the user, e.g., a software-defined radio (SDR).

The capability of controlling mmWave beam's steering angle from software enables a swathe of spectrum access and communication protocol possibilities. Advanced algorithms, implemented in software, can be used to perform mmWave beamforming for better communication efficiency [4]. In this paper, motivated by the need for connectability to an SDR platform, we design a patch array mmWave antenna. Fig. 1 shows how the overall SDR system architecture will work with the antenna. The SDR is connected to a PC via Ethernet port, with a sampling rate of up to 25 MHz.

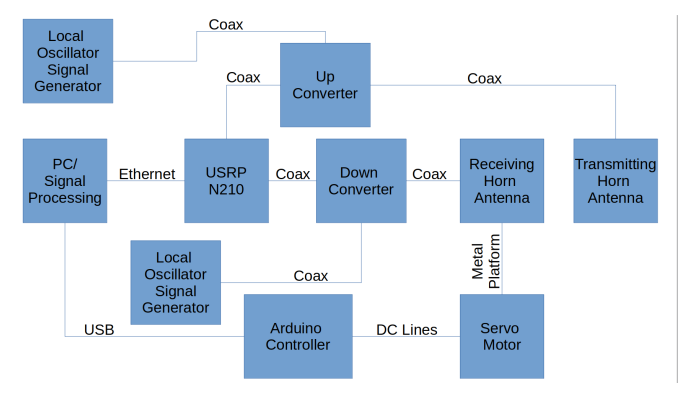


Fig. 1: SDR architecture

Digitally modulated signals generated by a signal generator are transmitted over the air via a mmWave (e.g., horn) antenna. The received signals are sampled by the SDR's Analog-to-Digital Converter (ADC). Customized software is used to store the sampled data. The user is able to electrically steer the antenna array through a micro-controller, which is used to drive Direct Current (DC) signals low and high, in order to select phase values from the digital phase shifters.

In recent years, patch array antennas are being designed for next generation mmWave test beds, [12]. There have been studies looking at design aspects of such array antennas for mmWave bands by mostly focusing on reducing their costs. Concepts being explored included novel feeding networks to patch elements [2], [10], use of shared elements for dualband operation at both sub-6 GHz and mmWave bands [5], and designs using multi-layer substrates [8] or integrated waveguides for dual-band operation [9]. These studies did not aim to offer an interface to an SDR platform, and hence, either did not include on-board phase shifters (that can be controlled by software) or limited the beamforming capability to few steering angles. The renowned testbed OpenMili [15], which planned for integration with SDR platforms, uses a 60 GHz four-element patch array antenna with one-bit phase shifters. Similarly, in [1], a phased array mmWave antenna was integrated with an SDR platform by using an analog phase shifter. Since these systems use only one-bit phase shifters, the phase sequencing is limited to two values, either 0° or 180°. As a result, these systems are limited to the number of beamforming radiated patterns that it can generate.

<sup>\*</sup> These authors contributed equally to this work.

In this paper, we design a four-element patch array antenna utilizing five-bit phase shifters, which allows for the sequencing of up to 25 phase values. This achieves a much greater number of radiated patterns, separable by 11.25°. Further, the antenna design is centered at 30 GHz frequency. The antenna elements are etched onto an RT Duroid 6002 board, which has a permittivity of 2.94 and a thickness of 0.254mm. The elements are spaced 0.6 wavelengths apart. The antenna design was simulated using ANSYS High Frequency Structure Simulator (HFSS) software. The design was able to achieve beamforming patterns from -36° to 36° with minimal side lobe interference. Moreover, the design was able to achieve bandwidths of hundreds of MHz. Main contributions of this work are as follows:

- We design a low-cost 30 GHz patch antenna design without a waveguide or cavity.
- Our antenna design attains 800 MHz of accessible bandwidth within very small dimensions (i.e., 3.6 mm×2.8 mm) and includes five 5-bit phase shifters yielding 2<sup>5</sup> phase values for beam steering.
- To integrate the phase shifters and provide an interface connectable to an SDR platform, we design feeding lines with minimal reflection and disturbance on the transmitted signals.

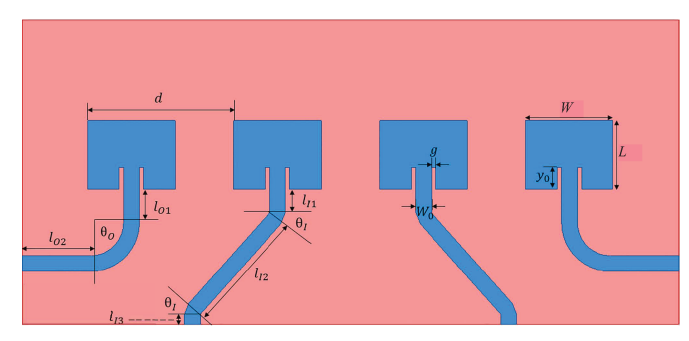


Fig. 2: Patch Antenna Array with Inset Feeding.  $d=6\ \mathrm{mm},$  $W_0 = 0.65$  mm, g = 0.1675 mm,  $y_0 = 0.9$  mm, W = 3.6mm, L = 2.8 mm,  $l_{O1} = 1.32$  mm,  $\theta_O = 90^{\circ}$ ,  $l_{O2} = 2.84$ mm,  $l_{I1} = 0.96$  mm,  $\theta_I = 45^{\circ}$ ,  $l_{I2} = 4.99$  mm,  $l_{I3} = 0.41$ mm.

### II. STEERABLE PATCH ARRAY ANTENNA DESIGN

### A. Patch Array Design

The array design begins with a simple patch antenna with inset feeding to achieve impedance matching at  $50\Omega$ . Fig. 2 shows the layout of the antenna array with dimensions. The patch antenna and feeding network are designed for operation at 30 GHz, with the array element spacing chosen to avoid grating lobes while providing a maximum steering angle of about  $\pm 36^{\circ}$  from boresight. Beam scanning is to be performed on the H-plane (L dimension in this case). The antennas are designed/simulated using copper for the antenna metal and ground plane, though in practice the copper will have a gold finish over the top to allow for wire bonding of the digital phase shifters. This will be further discussed in Section II-B. The dielectric substrate used is a 10-mil (0.254) mm) thick Rogers RT/duroid 6002 board with a dielectric constant of 2.94 for the substrate material.

Patch antennas are defined by their effective permittivity, patch width, and patch length [3]. The effective permittivity is a function of the relative permittivity, the width of patch, and the height of the substrate where antenna is being placed. The effective permittivity of the substrate material can be formulated as

$$\epsilon_{\text{eff}} = \frac{\epsilon_{\text{r}} + 1}{2} + \frac{\epsilon_{\text{r}} - 1}{2} \frac{1}{\sqrt{1 + 12\frac{H}{W}}},$$
(1)

where W is the patch width (m), H is the height of the substrate (m), and  $\epsilon_r$  is the relative permittivity of the substrate material (Farad per meter).

The patch width is a function of the speed of light, the center frequency (i.e., 30 GHz in our case), and the relative permittivity of the substrate. Hence, it can be expressed as

$$W = \frac{c}{2f_0\sqrt{\epsilon_{\rm r}}},\tag{2}$$

where c is the speed of light (m/s) and  $f_0$  is the center frequency (Hz). In a similar fashion, the patch length is expressed as

$$L = \frac{c}{2f_0\sqrt{\epsilon_{\text{eff}}}} - 0.824H \frac{(\epsilon_{\text{eff}} + 0.3)(\frac{W}{H} + 0.264)}{(\epsilon_{\text{eff}} - 0.258)(\frac{W}{H} + 0.80)}.$$
 (3)

The rectangular patch antenna inset feed length,  $y_0$ , is a function of the resonant resistance  $R_{in}$ . Deriving from the equivalent transmission line model [3], we can write the inset feed length as

$$y_0 = \arccos\left(\sqrt{\frac{50}{R_{\rm in}}}\right) \frac{L}{\pi}$$
 (4)

where the model is matched to 50 ohms input impedance, and  $R_{in}$  is a function of the conductances  $G_1$  and  $G_{12}$  in the following form:

$$R_{\rm in} = \frac{1}{2(G_1 + G_{12})}. (5)$$

 $G_1$  and  $G_{12}$  are derived from the radiated fields of the patch antenna cavity, integrated over 180 degrees [3] as

$$G_{1} = \frac{\int_{0}^{\pi} \left(\frac{\sin(\frac{k_{0}W\cos\theta}{2})}{\cos\theta}\right)^{2} (\sin\theta)^{3} d\theta}{120\pi^{2}}$$

$$G_{12} = \frac{\int_{0}^{\pi} \left(\frac{\sin(\frac{k_{0}W\cos\theta}{2})}{\cos\theta}\right)^{2} (\sin\theta)^{3} J_{0}(k_{0}L\sin\theta) d\theta}{120\pi^{2}}, (7)$$

$$G_{12} = \frac{\int_0^{\pi} \left(\frac{\sin(\frac{k_0 W \cos \theta}{2})}{\cos \theta}\right)^2 (\sin \theta)^3 J_0(k_0 L \sin \theta) d\theta}{120\pi^2}, (7)$$

where  $J_0$  is the Bessel function and  $k_0 = 2\pi/\lambda$  is the wave number for wavelength  $\lambda$  (m). Calculating the equations (1)-(7) in MATLAB, we obtained the patch width, the patch length, and the inset feed length as W=3.6 mm, L=2.8mm, and  $y_0 = 0.99$  mm. When simulating the antenna design in HFSS, we tuned the inset feed to  $y_0 = 0.9$  mm.

### B. Phase Shifters for SDR Interface

The digital phase shifters used are the TGP2100 30 GHz 5-bit digital phase shifter. This allows for selection of phases from  $0^{\circ}$  to  $360^{\circ}$  with increments of  $11.25^{\circ}$ . Fig. 3 shows an image of the phase shifter; at 30 GHz it has an insertion loss of 7dB with an RMS amplitude error of 0.5 dB.

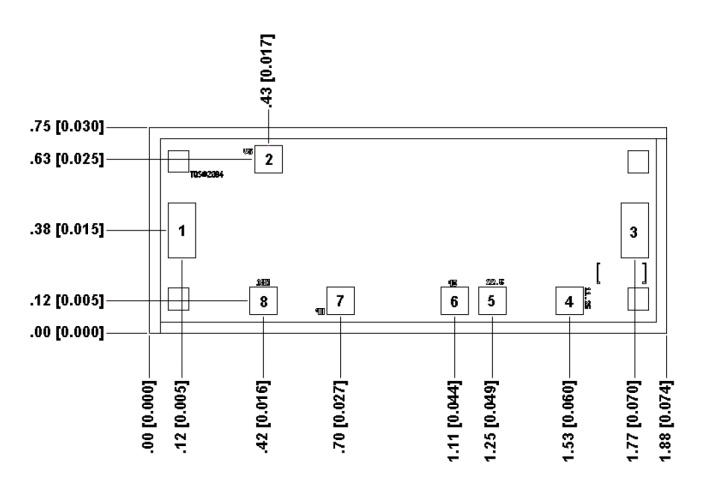


Fig. 3: Physical layout of the phase shifter showing dimensions along the chip as mm[inches]. Total chip dimensions:  $1.88 \times 0.75 \times 0.1 \text{ mm}$ 

Due to the small size of the phase shifters, they will be mounted onto the board via wire bonding with gold wire. This requires that the top metal of the board be finished with gold, since the phase shifter pads are gold. One end of wire will be connected to each of the terminals on the phase shifter, 5 bits and one reference. The other end of each of those wires will connect to pads on the board which connect to DC feeding lines that run to surface mounted pins that connect to an off-board SDR module that will digitally control the phase shifting. Making use of the fact that the phase shifters are reciprocal allows the DC bias lines to also be designed symmetrically, as shown in Fig. 4.

# C. Feeding Network

The feeding network of this design presented an interesting challenge. The antennas are equally spaced 6 mm apart, but the 2.92 mm connectors are each 12.7 mm wide. Because of this the RF feeding lines need two different types of lines. One type for the outer lines and another for the inner lines. To maintain the same phase from the 2.92 mm connectors to the phase shifters, the lines must have the same electrical length. In addition, at the millimeter-wave frequency the feeding lines cannot be too long, or else they behave as radiative elements as well, and make beam steering impossible. To combat this, the connectors are spaced such that the minimal feeding line lengths can be achieved by having two connectors on the east and west sides of the board and two connectors on the south side of the board. The outer line must bend from the outermost antennas outward towards the connectors. The simplest way to accomplish this is with

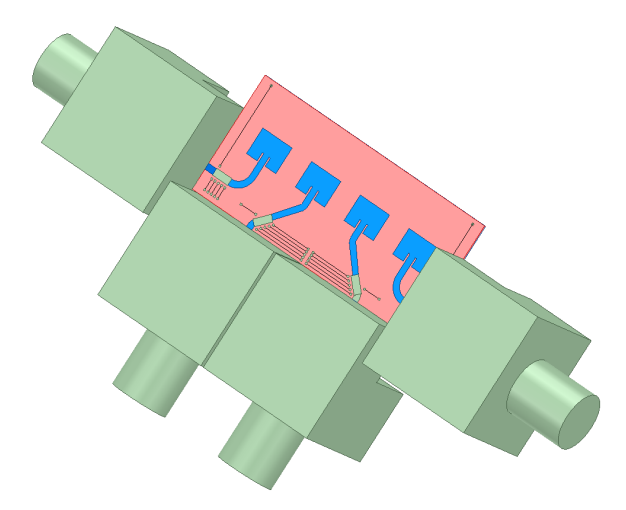


Fig. 4: Schematic of the entire structure including 2.92 mm connectors, phase shifters, and DC biasing lines.

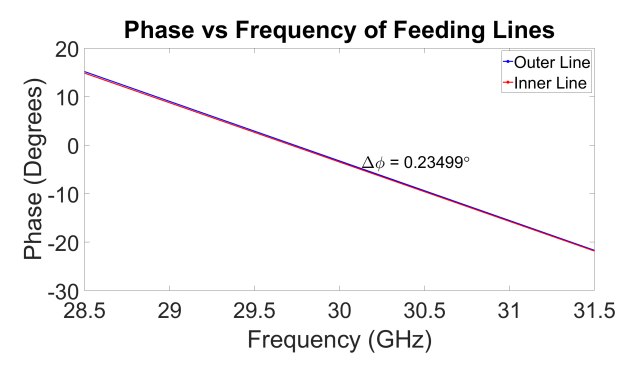
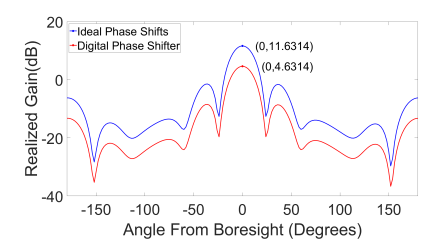


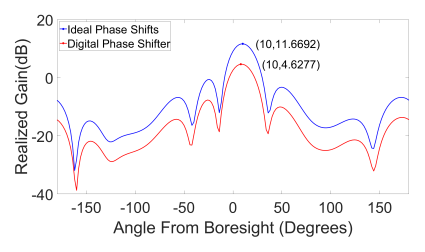
Fig. 5: Plot of the phase difference vs. frequency of the two transmission lines.

a 90 degree bend towards the east and west edges of the board. This gives enough room for the connectors and DC bias lines. The inner line follows a near straight path down, with two 45 degree bends that allow for adequate connector spacing on the southern edge of the board. Due to parasitic capacitance from the bends the inner lines' straight segments must be fine tuned so that the phase is equal to the outer lines. Fig. 2 presents the layout of the design with the feeding lines included and the dimensions displayed. An analysis of the phase is shown in Fig. 5 showing the design does achieve a phase error of about  $0.23^{\circ}$ . The lines are relatively short, totaling just over 1 guided wavelength long each ( $\lambda_g = 6.5$  mm).

#### III. SIMULATION SETUP AND RESULTS

The transmission lines and antenna array are combined into a structure that does not physically include the phase shifters or DC bias lines as shown in Fig. 2. The effects of the phase shifters are discussed further in Section II-A, but for the simulation the effects can be approximated in post-processing, and the setup does not require the phase shifters to be included. Likewise, the connectors are simulated using





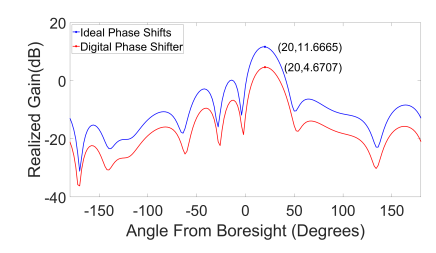
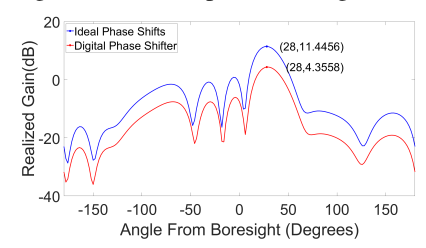
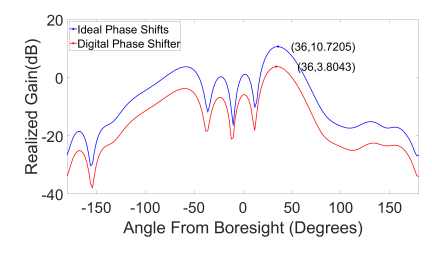


Fig. 6: Radiation pattern and gain at 0°. Fig. 7: Radiation pattern and gain at 10°. Fig. 8: Radiation pattern and gain at 20°.





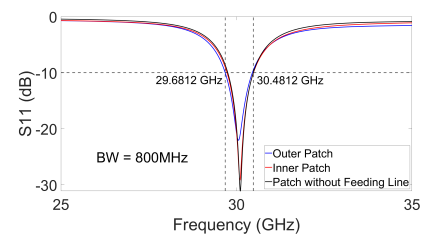
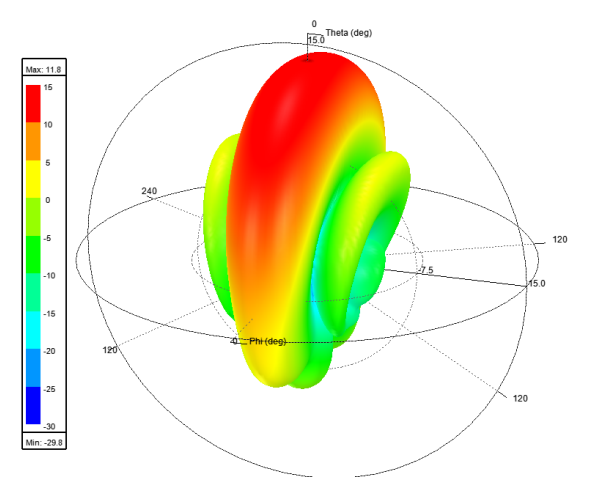
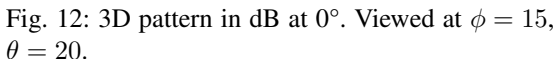


Fig. 9: Radiation pattern and gain at 28°. Fig. 10: Radiation pattern and gain at 36°.

Fig. 11: S11 plot of one element.





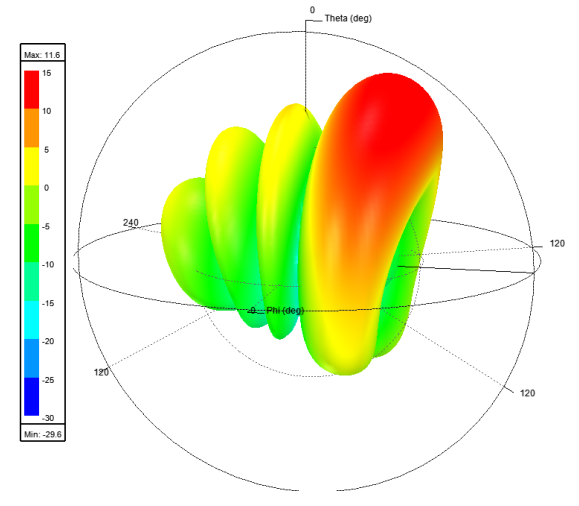


Fig. 13: 3D pattern in dB at 30°. Viewed at  $\phi=15,$   $\theta=20$ 

lumped ports, and the spacing between the lines is kept as if the real connectors were placed on the board.

#### A. Gain

The antenna array is able to achieve a maximum realized gain of 12.35 dB, but this becomes reduced due to the digital phase shifters' insertion loss. Figs. 6-10 show plots of the radiation patterns at different angles from boresight to 36 degrees. Included in each figure is also a comparison of the pattern when using the digital phase shifter (both its loss and the angle offsets it can provide are taken into account). From these plots it can be seen that by using the digital phase shifters, the steering angle error due to phase error from the phase shifter is negligible, and the beam can be comfortably steered over a fairly wide range without encountering grating lobes. Further, the loss due to the phase shifters and feeding network is around 7dB, which is dominated by the insertion

loss of the phase shifters, indicating that the feeding network adds negligible loss to the design. We also show the 3D radiation patterns in Figs. 12 and 13 with 0° and 30° steering angles, respectively. As expected, the lobes above and below the boresight plane are smaller and consistently shrinking as moving away from the boresight plane.

### B. S11 Plot and Bandwidth

The S11 of each element in the antenna array is affected by the feeding network. Fig. 11 shows that there is very little difference between the performance when the feeding network is introduced. Only two traces out of the four are shown for the elements with feeding lines since the design is symmetrical and S11 = S33; S22 = S44. Similar to the gain plots, we observe around 7dB loss at the operational frequency of the antenna when the impact of all components on the board are accounted. The antenna array achieves a

maximum bandwidth of around 800 MHz. The bandwidth is largely unaffected by the feeding network and remains consistent throughout the beam scanning.

#### IV. SUMMARY AND FUTURE WORK

A low-cost design for a beam-steerable patch antenna array for SDR platforms is presented. The simulation results demonstrate a high-directivity array with beam-steering capability. At a center frequency of 30 GHz, 2.7% fractional bandwidth, 5.35 dBi gain, and beam-steering from -36° to 36° are achieved. As a result of integrating the feeding network, the power and control of the device components is done through a low-cost low-loss method with negligible impact on the performance. When combined with 5-bit digital phase shifters, the beam-steering can be done through SDR platforms with negligible phase error; and, as a result, the fabrication costs, complexity, and size of the design have been greatly reduced.

Future work on this design includes fabrication and testing of the patch antenna array, both with physical antenna measurements and testing with the SDR interface. The fabrication process, including wire bonding of the digital phase shifters, is a necessary and non-trivial step that must be taken due to the small size of the components that operate at 30 GHz. The array presented will also be fabricated multiple times, creating a set of arrays that will be used to achieve omnidirectionality in the entire setup.

Several future directions can be pursued. Considering the presence of on-board digital phase shifters and the necessary feeding network to SDR ports, a new antenna geometry can be explored. This would include different types of antennas as the array elements which can provide higher gain, or increasing the number of elements to also increase gain.

#### ACKNOWLEDGMENT

This work was supported in part by U.S. National Science Foundation award 2115215.

## REFERENCES

- [1] O. Abari, H. Hassanieh, M. Rodreguiz, and D. Katabi. Poster: A millimeter wave software defined radio platform with phased arrays. In *Proceedings of ACM Annual International Conference on Mobile Computing and Networking (MOBICOM)*, page 419–420, New York, NY, USA, 2016.
- [2] A. Abbaspour-Tamijani and K. Sarabandi. An affordable millimeterwave beam-steerable antenna using interleaved planar subarrays. *IEEE Transactions on Antennas and Propagation*, 51(9):2193–2202, 2003.
- [3] C. A. Balanis. Antenna theory: Analysis and design. John wiley & sons, 2015.
- [4] J. Chen, W. Feng, J. Xing, P. Yang, G. E. Sobelman, D. Lin, and S. Li. Hybrid beamforming/combining for millimeter wave mimo: A machine learning approach. *IEEE Transactions on Vehicular Technology*, 69(10):11353–11368, 2020.
- [5] X.-H. Ding, W.-W. Yang, W. Qin, and J.-X. Chen. A broadside shared-aperture antenna for (3.5, 26) GHz mobile terminals with steerable beam in millimeter wave band. *IEEE Transactions on Antennas and Propagation*, pages 1–1, 2021.
- [6] S. Ghosh and D. Sen. An inclusive survey on array antenna design for millimeter-wave communications. *IEEE Access*, 7:83137–83161, 2019.

- [7] W. Hong, Z. H. Jiang, C. Yu, J. Zhou, P. Chen, Z. Yu, H. Zhang, B. Yang, X. Pang, M. Jiang, Y. Cheng, M. K. T. Al-Nuaimi, Y. Zhang, J. Chen, and S. He. Multibeam antenna technologies for 5G wireless communications. *IEEE Transactions on Antennas and Propagation*, 65(12):6231–6249, 2017.
- [8] N. S. Jeong, Y.-C. Ou, A. Tassoudji, J. Dunworth, O. Koymen, and V. Raghavan. A recent development of antenna-in-package for 5G millimeter-wave applications (invited paper). In *Proceedings of IEEE Wireless and Microwave Technology Conference (WAMICON)*, pages 1–3, 2018.
- [9] J. Lan, Z. Yu, and J. Zhou. A 3.5/28 GHz beam-steerable shared-aperture antenna based on shorting-vias-loaded patch. In *Proceedings of IEEE MTT-S International Wireless Symposium (IWS)*, pages 1–3, 2020.
- [10] Y. Liu, O. Bshara, I. Tekin, and K. R. Dandekar. A 4 by 10 series 60 GHz microstrip array antenna fed by butler matrix for 5G applications. In *Proceedings of IEEE Wireless and Microwave Technology Conference (WAMICON)*, pages 1–4, 2018.
- [11] G. Mumcu, M. Kacar, and J. Mendoza. Mm-Wave beam steering antenna with reduced hardware complexity using lens antenna subarrays. IEEE Antennas and Wireless Propagation Letters, 17(9):1603–1607, 2018
- [12] A. Quadri, H. Zeng, and Y. T. Hou. A real-time mmwave communication testbed with phase noise cancellation. In *Proceedings of IEEE Conference on Computer Communications (INFOCOM) Workshops*, pages 455–460, 2019.
- [13] S. Seth, H. Yazdani, M. Yuksel, and A. Vosoughi. Rate-optimizing beamsteering for line-of-sight directional radios with random scheduling. In *Proceedings of IEEE International Symposium on Dynamic* Spectrum Access Networks (DySPAN), pages 53–60, 2021.
- [14] J. Zhang, X. Ge, Q. Li, M. Guizani, and Y. Zhang. 5G millimeter-wave antenna array: Design and challenges. *IEEE Wireless Communications*, 24(2):106–112, 2017.
- [15] J. Zhang, X. Zhang, P. Kulkarni, and P. Ramanathan. OpenMili: a 60 GHz software radio platform with a reconfigurable phased-array antenna. pages 162–175, 10 2016.